Theory of Surface Plasmons of the Alkali-Adatom-Chain Model on Si(100)2×1 Surfaces

Masaru Tsukada, Hiroshi Ishida, and Nobuyuki Shima
Department of Physics, University of Tokyo, Hongo, Bunkyo-ku, Tokyo 113, Japan
(Received 21 March 1984)

With the use of the random-phase approximation, we obtained the dispersion relation of the inter- and intra-surface-band plasmon of the parallel-rod model, which simulates the alkali-metal adatom chains on Si(100)2×1 surfaces. There are two interband plasmon modes: One corresponds to the polarization vertical to the surface and the other to the polarization vertical to both the rod axis and the surface normal. The results explain fairly well the plasmon modes of the Si(100)(2×1)K surface observed recently.

PACS numbers: 73.90.+f, 79.20.−m

It has been observed that alkali-metal adatoms over Si(100)2×1 surfaces show many interesting properties.[1,2] For example, the adlayer with lower coverages has the character of an insulator, while beyond certain critical coverage it changes to metallic.

The work function decreases and increases with the coverage in the insulating regime and in the metallic regime, respectively. Based on the low-energy electron-diffraction observation, the alkali-metal adatoms are found to sit on the sites over raised rows of the "dimers" of the Si(100)2×1 surfaces.[3] At the saturation coverage infinitely long chains of the alkali-metal adatoms are completed which extend in the [110] direction.

A characteristic electron-energy-loss spectroscopy peak has been observed in the metallic coverage region, which is due to the plasmon excitation of the adlayer. The abrupt increase of the intensity with the coverage θ starts around the coverage where the adlayer changes from insulator to metal.[1,2] Very recently, the dispersion relation of the surface plasmon has been measured with AREELS (angle-resolved electron-energy-loss spectroscopy) by Aruga, Tochihara, and Murata[4] on Si(100)(2×1)K surfaces. They found a major plasmon peak with a finite energy in the limit of the wave number $\vec{Q}\to 0$. The plasmon energy seems not to decrease with $\vec{Q}$ even in the small-$\vec{Q}$ region. This behavior is different from that observed for Ni(100)-K surfaces,[5] and unexpected by Newns's theory[6] for a uniform metallic thin film. Moreover, Aruga, Tochihara, and Murata found a shoulder in the tail of the main peak, which indicates the presence of different excitation modes.[4] Some general properties of the plasmon dispersion of the metallic adlayer in the small-$\vec{Q}$ region are discussed by Nakayama.[7] It seems that the dispersion relation and the oscillator strength of the excitation modes depends crucially on the peculiar structure of the adlayer. Since there have been no theoretical works for the collective excitation modes of the array of metallic adatom chains, we calculate the plasmon dispersion relation for general $\vec{Q}$ regions using the simplified model described below.

As shown in Fig. 1, the model consists of uniform square rods confining free electrons. The side length l is chosen as 7.0 a.u., which is close to the K-K distance (7.2 a.u.) in the chain. Each rod is assumed to include one electron per length l. The separation a of the two adjacent rods is 14.6 a.u., which is determined by the structure of the Si substrate.[3] The substrate of Si is modeled by the uniform semi-infinite dielectric medium with the dielectric constant κ.

The eigenfunction and the energy of the electrons confined in the nth rod is written as

$$\phi_{k,n}^{p,q}=\frac{2}{l\sqrt{L}}e^{ikx}\sin\left[\frac{p\pi}{l}(y-na)\right]\sin\left[\frac{q\pi}{l}z\right] \quad (1)$$

and

$$\epsilon_k^{p,q}=\frac{k^2}{2m}+\frac{1}{2\mu}\left[\left(\frac{p\pi}{l}\right)^2+\left(\frac{q\pi}{l}\right)^2\right]. \quad (2)$$

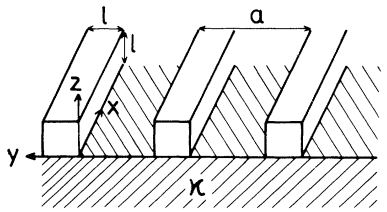

FIG. 1. The parallel-rod model which consists of the uniform square rods confining free electrons on the uniform semi-infinite dielectric medium with the dielectric constant κ (shaded region). The axes directions are also shown.

In the above m is the free-electron mass and μ is the effective mass for vertical directions (y,z) to the rod axis. μ is an adjustable parameter to be determined as shown below. The integers p,q minus unity mean the number of nodes of the wave function in y and z directions, respectively. We include only the following modes, $(p,q)=(1,1)$, $(2,1)$, $(1,2)$, each corresponding to K $4s$, $4p_y$, $4p_z$ orbitals, respectively. The higher-energy bands $\epsilon_k^{2,1}$ and $\epsilon_k^{1,2}$ are assumed to be empty, while the lowest one $\epsilon_k^{1,1}$ is assumed to be partially occupied.

The induced charge $\rho_{\rm ind}(\vec{r},\omega)$ due to the external charge $\rho_{\rm ext}(\vec{r},\omega)$ is obtained by the standard random-phase approximation as follows:

$$\rho_{\rm ind}(\vec{r},\omega)=2\sum_{i,j}\frac{f_i-f_j}{\epsilon_i-\epsilon_j+\omega+i\delta}\phi_i^*(\vec{r})\phi_j(\vec{r}) \times\int d\vec{r}'\int d\vec{r}''\phi_i(\vec{r}')\phi_j^*(\vec{r}')G(\vec{r}',\vec{r}'')[\rho_{\rm ext}(\vec{r}'',\omega)+\rho_{\rm ind}(\vec{r}'',\omega)], \tag{3}$$

where f_i,f_j are the Fermi distribution functions and the subscripts i,j represent the set of indices k,n,p,q. The function $G(\vec{r},\vec{r}')$ represents the potential at $\vec{r}$ induced by a unit point charge at $\vec{r}'$ in the semi-infinite dielectric medium;

$$G(\vec{r},\vec{r}')=\frac{\Theta(z')}{|\vec{r}-\vec{r}'|}-\frac{\kappa-1}{\kappa+1}\frac{\Theta(z')}{[|\vec{\rho}-\vec{\rho}'|^2+(z+z')^2]^{1/2}}+\frac{2}{\kappa+1}\frac{\Theta(-z')}{|\vec{r}-\vec{r}'|}. \tag{4}$$

In the above Θ is the usual step function and $\vec{\rho},\vec{\rho}'$ are the (x,y) components of the position vector.

The inverse of the dielectric function $\epsilon(\vec{Q},\omega)$ can be obtained by the Fourier coefficient $\varphi_{\rm ind}(\vec{Q},\omega)$ of the field due to $\rho_{\rm ind}(\vec{r},\omega)$ plus the image field of the substrate as follows:

$$\frac{1}{\epsilon(\vec{Q},\omega)}=\frac{\varphi_{\rm ind}(\vec{Q},\omega)}{\varphi_{\rm ext}(\vec{Q},\omega)}+1=1+\frac{1}{aL}\left(\frac{l}{2}\right)^2\vec{Q}^2\sum_{\nu=1}^{3}\beta^*(\vec{Q},\nu)J^*(\vec{Q},\nu)F(Q_x,\nu,\omega)D(\vec{Q},\nu,\omega), \tag{5}$$

where $\varphi_{\rm ext}(\vec{Q},\omega)$ is the Fourier coefficient of the external field. The factor $\beta(\vec{Q},\nu)J(\vec{Q},\nu)$ represents the matrix element of the field due to the external charge component $\exp(i\vec{Q}\cdot\vec{r})$ between the states $\phi_{kn}^{p_1q_1}$ and $\phi_{k-Q_x n}^{p_2q_2}$, where the pair-band indices p_1,p_2,q_1,q_2 are specified by the mode index ν as shown in Table I. The quantities $\beta(\vec{Q},\nu)$ and $J(\vec{Q},\nu)$ are written as

$$\beta(\vec{Q},\nu)=\frac{2}{l}\int_0^l dy\,\exp(iQ_y y)\sin\left(\frac{p_1\pi y}{l}\right)\sin\left(\frac{p_2\pi y}{l}\right), \tag{6}$$

$$J(\vec{Q},\nu)=\frac{8}{l^2\vec{Q}^2}\int_0^l dz\,\sin\left(\frac{q_1\pi z}{l}\right)\sin\left(\frac{q_2\pi z}{l}\right)\left(e^{iQ_z z}-\frac{\kappa-1}{\kappa+1}e^{-|\vec{Q}_\parallel|z}\right), \tag{7}$$

with $\vec{Q}_\parallel=(Q_x,Q_y)$, where p_1, p_2, q_1, and q_2 are determined by ν. The interband polarization function $F(Q,\nu,\omega)$ $(\nu=2,3)$ is defined as

$$F(Q,\nu,\omega)=\frac{2\pi}{L}\sum_k\frac{f_{k-Q}^{q_2p_2}-f_k^{q_1p_1}}{\epsilon_{k-Q}^{q_2p_2}-\epsilon_k^{q_1p_1}+\omega+i\delta}+\frac{2\pi}{L}\sum_k\frac{f_{k-Q}^{q_1p_1}-f_k^{q_2p_2}}{\epsilon_{k-Q}^{q_1p_1}-\epsilon_k^{q_2p_2}+\omega+i\delta}, \tag{8}$$

where f_k^{qp} is the Fermi distribution function. The intraband polarization function $F(Q,\nu,\omega)$ $(\nu=1)$ is defined as the first term of the right-hand side of Eq. (8). The function $D(\vec{Q},\nu,\omega)$ in Eq. (5) is the matrix element of the total field between the pair-band states and is obtained by

$$\sum_{\nu'=1}^{3}[\delta_{\nu\nu'}-\sum_{\vec{G}}\beta(\vec{Q}+\vec{G},\nu)I(\vec{Q}+\vec{G},\nu\nu')\beta^*(\vec{Q}+\vec{G},\nu')F(Q_x,\nu',\omega)]D(\vec{Q},\nu',\omega)=\beta(\vec{Q},\nu)J(\vec{Q},\nu), \quad \nu=1,2,3 \tag{9}$$

$$\vec{G}=\left(0,\frac{2\pi n}{a},0\right), \quad n=0,\pm1,\pm2,\ldots. \tag{10}$$

In the above $I(\vec{Q},\nu\nu')$ is defined by

$$I(\vec{Q},\nu\nu')=\left(\frac{2}{l}\right)^2\frac{z}{a|\vec{Q}_{\parallel}|}\int_0^l dz\int_0^l dz'\sin\left(\frac{q_1\pi z}{l}\right)\sin\left(\frac{q_2\pi z}{l}\right)$$
$$\times\left(e^{-|\vec{Q}_{\parallel}||z-z'|}-\frac{\kappa-1}{\kappa+1}e^{-|\vec{Q}_{\parallel}||z+z'|}\right)\sin\left(\frac{q_1'\pi z'}{l}\right)\sin\left(\frac{q_2'\pi z'}{l}\right), \quad (11)$$

with the indices q_1,q_2 and q_1',q_2' corresponding to ν and ν', respectively.

The plasmon energies are given as the zero points of the determinant of the coefficient matrix of Eq. (9). There are three coupled plasmon modes; the $4s$ intraband mode ($\nu=1$), and the $4s$-$4p_y$ ($\nu=2$), and $4s$-$4p_z$ ($\nu=3$) interband modes. The strength of each component in the three modes is determined by $D(\vec{Q},\nu,\omega)$. Figure 2 shows the dispersion relation of the three modes for the case in which the angle θ between $\vec{Q}_{\parallel}$ and the rod axis equals $\pi/4$. The dielectric constant of the Si substrate is assumed to be $\kappa=15$. The lowest mode ω_1 shown by the dashed-dotted line almost comes from the intraband mode in the small-$|\vec{Q}_{\parallel}|$ region. The dashed curve and the heavy solid curve represent the interband collective modes, $4s$-$4p_y$ (ω_2) and $4s$-$4p_z$ (ω_3) for the small-$|\vec{Q}_{\parallel}|$ region, respectively. The shaded regions correspond to the intraband and the interband individual excitations. The observed peak energies of AREELS are also plotted in the figure. The energy difference $\omega_{12}=(\pi/l^2)/2\mu$ between the excited and the lowest bands is adjusted to 0.59 eV in order that ω_2 and ω_3 roughly reproduce the AREELS peak energy for $\vec{Q}_{\parallel}\rightarrow 0$. Our preliminary calculations by the linear combination of atomic orbitals, thin-film method indicate that $\omega_{12}\cong 0.4$–0.8 eV.

Reflecting the one-dimensional character of the system, the plasmon energy is determined almost by the component of the wave vector parallel to the rod axis. Hence the dispersion relation for general θ is similar to that for $\theta=\pi/4$ (Fig. 2) with the abscissa multiplied by $\cos(\pi/4)/\cos\theta$. This feature can be clearly seen in the observed AREELS[4] by the comparison between the dispersions of the main loss peak corresponding to the [110] and [100] azimuth directions.

The slope of the dispersion curve of the ω_3 mode at $|\vec{Q}_{\parallel}|=0$ is slightly negative. But the negative dispersion is limited only in a very small region of $|\vec{Q}_{\parallel}|$ in contrast to those experimentally found for alkali-metal overlayer on metal surfaces. On the other hand, the ω_2 mode has a positive dispersion at $|\vec{Q}_{\parallel}|=0$ and its energy is close to that of the ω_3 mode. The presence of the ω_2 mode is a characteristic feature of the peculiar chain structure of the overlayer, since this mode, due to the polarization for the vertical direction to both the chain axis and the surface normal, does not exist for the uniform two-dimensional adlayer. It should be noted that

TABLE I. Correspondence of the mode index ν and the sub-band indices p_1,p_2,q_1,q_2.

ν	Mode	p_1	p_2	q_1	q_2
1	$4s$-$4s$	1	1	1	1
2	$4s$-$4p_y$	1	2	1	1
3	$4s$-$4p_z$	1	1	1	2

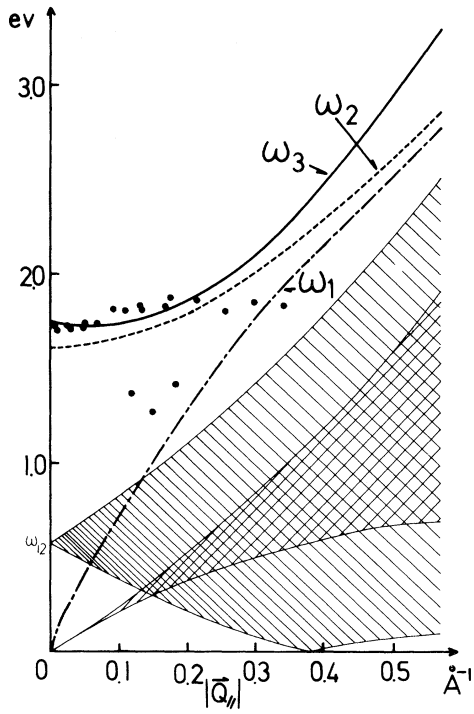

FIG. 2. Energy dispersions of the overlayer plasmons for the case of $\kappa=15$ and $\theta=\pi/4$. The dashed-dotted, dashed, and heavy solid lines correspond to the ω_1, ω_2, and ω_3 modes, respectively. The intra- and the interband individual excitations are possible in the shaded regions.

the energy of the ω_2 mode at $|\vec{Q}_{\parallel}| \rightarrow 0$ is pushed up at a higher energy position than the individual interband transition energy ω_{12} due to the depolarization effect caused by the umklapp process. This effect is taken to into account in the present theory by the summation over the reciprocal lattice $\vec{G}$ in the left-hand side of Eq. (9).

The main peak of the AREELS observed by Aruga, Tochihara, and Murata[4] might be contributed by the ω_2 and ω_3 modes of the alkali-metal overlayer, since the energies of the two modes are so close to each other. The excitation intensity of the ω_2 mode is calculated to be considerably smaller than those of ω_1 and ω_3 modes. However, for a more realistic model including the orbital hybridization with Si, the intensity of the ω_2 mode might be more enhanced. This point will be discussed in a forthcoming paper. The excitation mode observed as the shoulder on the low-energy side of the main EELS peak corresponds well to the intraband mode. The appearance of the intraband mode with its characteristic energy dispersion is evidence of the one-dimensional metallic character of the overlayer.

In conclusion, the dispersion relations of the interband plasmons (ω_2 and ω_3) for the parallel-rod model agree satisfactorily with that of the main loss peak observed by AREELS for Si(100)-(2×1)K surface. The ω_2 mode peculiar to the chain overlayer structure has positive linear dispersion at $|\vec{Q}_{\parallel}| = 0$ in accord with the behavior of the dispersion of the observed AREELS peak. The ω_3 mode has a slightly negative dispersion at $|\vec{Q}_{\parallel}| = 0$. But the dispersion might change to positive for a more realistic model including the orbital hybridization with the Si substrate.[7] We may conclude at least that the overlayer plasmon mode of Si(100)(2 ×1)K surface does not show any strong negative dispersion in contrast to the case of the uniform two-dimensional alkali-metal overlayer on metals.[5] Subsidiary structure in the tail of the main loss peak can be explained by the intraband plasmon (ω_1) reflecting metallic character along the rod axis.

The authors would like to express their sincere thanks to Professor Y. Murata, Dr. H. Tochihara, Dr. T. Aruga, and Professor M. Nakayama for helpful and stimulating discussions and showing them their results prior to publication. This work was partially supported by the Grant-in-Aid from the Ministry of Education.

[1]H. Tochihara and Y. Murata, J. Phys. Soc. Jpn. **51**, 2920 (1982).

[2]H. Tochihara, Surf. Sci. **126**, 523 (1983).

[3]J. D. Levine, Surf. Sci. **34**, 90 (1973).

[4]T. Aruga, H. Tochihara, and Y. Murata, preceding Letter [Phys. Rev. Lett. **53**, 372 (1984)].

[5]U. Jostell, Surf. Sci. **82**, 333 (1979).

[6]D. M. Newns, Phys. Lett. **38A**, 341 (1972).

[7]M. Nakayama, Solid State Commun. (to be published).